Palladium clusters on graphite: Evidence of resonant hybrid states in the valence and conduction bands

M. Cini, M. De Crescenzi, F. Patella, N. Motta, M. Sastry, F. Rochet,*
R. Pasquali, and A. Balzarotti
Dipartimento di Fisica, Università di Roma II, Via E. Carnevale, I-00173 Roma, Italy

C. Verdozzi
Istituto Metodologie Avanzate Inorganiche, Consiglio Nazionale delle Ricerche, I-00016 Monterotondo Scalo, Roma, Italy
(Received 11 October 1989)

The electronic structure of Pd clusters deposited on polycrystalline graphite has been investigated by x-ray photoemission, Auger spectroscopy, and bremsstrahlung isochromat spectroscopy. Initial- and final-state shifts of energy levels as a function of the average cluster size R are small, but important modifications of the density of filled and empty states at the Fermi level are observed. With decreasing particle size, the d portion of the conduction band broadens and shifts to higher energy while its valence counterpart shows the opposite shift. A simple analytical model is developed which accounts in some detail for the measured shifts and linewidths and also explains earlier x-ray-absorption data. The size dependences are explained in terms of mixing of Pd $4d$ and graphite π^* continua with a squared coupling constant V^2 proportional to R^{-1}. As a consequence a gap opens up across the Fermi level in the cluster density of states and unoccupied hybrid resonances arise as observed experimentally. Initial-state energy shifts and cluster charging are estimated and found to play a minor role for the present system.

I. INTRODUCTION

The size-dependent electronic structure of metallic clusters is a challenging field that has received in the last few years renewed theoretical and experimental interest.[1-7] Changes of the energy position and width of the structures are observed in the valence band, core levels, and conduction states of the metal particles as a function of their size. These changes have been discussed in terms of initial- and/or final-state effects due to differences in the potential experienced by atoms in bulk metal and in small clusters where metallic properties are reduced and the electronic levels approach those of an isolated atom.[4,8-10] Ionizing spectroscopies such as x-ray photoemission (XPS), Auger electron spectroscopy (AES), and bremsstrahlung isochromant spectroscopy (BIS) leave a charge on the clusters whose contribution to the polarization energy is partially screened by the substrate when particles are supported. Finally, the one-hole local density of states (LDOS) might, in principle, change in a complex way with reducing particle size because of the increased number of surface and edge atoms.[11]

At present a large number of experimental results is available on different systems. In the case of Ag clusters deposited on amorphous carbon (partially conducting) substrate, the same shift to higher binding energy occurs for the core levels, the centroid of the valence d band, and the Fermi-level (E_F) position with decreasing cluster size.[3] Core-level shifts were observed for Sn clusters deposited on amorphous carbon while they were absent for the same Sn coverages on metallic glasses.[9] This evidence may support the relevance of cluster charging effects. However, for Cu aggregates deposited on crystalline and amorphous carbon, the centroids of the valence band and the core level do not undergo the same energy displacement and the bandwidth remains unaltered independently of the nature of the substrate.[6] Moreover, narrowing and shift of the valence d band have also been found on a variety of thin metallic films deposited on metallic substrates[12-15] where size effects due to charging cannot be present. Differences in bulk and cluster initial states and relaxation energies have been invoked to interpret photoemission spectra of metal aggregates on various semiconductors including Pd clusters on amorphous carbon substrates.[4]

In this work a combined theoretical and experimental study of the electronic structure of palladium clusters deposited on graphite as a function of the particle size is presented. Filled and empty states have been examined by using XPS, AES, and BIS. A theoretical model is developed which is able to include the essential features of a very complicated situation in a simple analytical form. The model fully accounts for the qualitative trends observed in all the spectroscopies, including earlier x-ray-absorption near-edge structure (XANES) results[5] and it also provides, to some extent, quantitative estimates. We find that initial- and final-state shifts are quite small for Pd clusters on graphite and the inhomogeneous broadening of the single-particle density of states due to the cluster size distribution also plays a minor role in this system. The potential experienced by an electron above E_F is rather flat and, in the absence of large potential bar-

riers, the electron lifetime inside the cluster is close to the semiclassical transit time. This produces a very effective mixing of the Pd $4d$ and graphite π^* continua which can be described by a squared coupling constant V^2 proportional to R^{-1}, where R is the average cluster size. The mixing produces hybrid resonant states above the Fermi level that are accessible both for the decay of an electron added to the system, as in BIS, and for an x-ray-absorption process (XANES). A gap develops across E_F with decreasing cluster size, and the Pd valence d band becomes filled. XPS features induced by interatomic relaxation are suppressed, while the intra-atomic correlations leave the Auger profile substantially unchanged. This paper is organized as follows. In Sec. II we give details on the experimental system and on the preparation and characterization of the Pd clusters. The theoretical formalism is introduced in Sec. III and applied to derive the bulk Pd bands (Sec. III A). In Sec. III B we discuss hole-hole interactions in the clusters. The qualitative trends expected for Pd clusters on graphite, as function of size, are illustrated in Sec. III C using a simplified form of the Pd LDOS. Section IV presents a detailed comparison of the XPS, AES, BIS, and XANES spectra with the results of the model using the more realistic Christensen theoretical LDOS (Ref. 16) for Pd.

II. EXPERIMENTAL DETAILS

Combined BIS, AES, and XPS measurements were performed in an UHV system (10^{-10}-Torr range) on *in situ* grown samples. The apparatus for the BIS measurements consisted of a high-current Vacuum Generator LEG32 electron gun ($I_{\max}=500\ \mu A/cm^2$) and a modified $\frac{1}{2}$-meter x-ray monochromator (grating size $50\times50\ mm^2$) set for detection of the 1486.6-eV radiation. A channeltron, coated by MgF_2 to increase x-ray detection efficiency, was used as detector. BIS spectra with a good signal-to-noise ratio were collected within 30 min having a counting rate at the threshold of about 100 counts/s. The energy resolution of the incident electron beam (0.9 eV) and of the x-ray monochromator (0.6 eV) determined the Gaussian broadening $\sigma=1.1$ eV of the experimental data.

XPS and AES spectra were collected on the same samples with the use of nonmonochromatized Al $K\alpha$ radiation (1486.6 eV) and a hemispherical electron analyzer with a total resolution comparable to that of BIS measurements.

A. Sample preparation

Successive evaporations of Pd have been performed in ultrahigh-vacuum conditions ($<10^{-9}$ Torr) on clean polycrystalline graphite substrates (Goodfellow, 99.99% purity), to form metallic aggregates with increasing mean diameter until the formation of a continuous film. The amount of metal deposited was measured with a quartz microbalance. The surface of graphite was previously cleaned by heating at $T=400$ °C in UHV in order to remove any contaminant and then held at room temperature during the Pd evaporation.

It is well known that the cluster mean diameter is very difficult to evaluate using spectroscopies that average the physical information on a large sample area. The standard procedure applied is to follow the relative photoemission intensities of the C $1s$ and Pd $3d$ core levels and their associated Auger transitions. However, while it is possible to distinguish among different growths (layer by layer, intermixing, island formation), the detailed information on the morphology, size distribution, and number of nucleation sites cannot be derived. Several simple models have been proposed for noble and near noble metals on various substrates, which relate the mean cluster diameter to the amount of metal deposition. In Fig. 1 we show, as a function of the nominal thickness, the percentage signal for C $1s$ and Pd $3d$ core lines each normalized by its XPS sensitivity factor. The observation of the graphite signal at high Pd coverages is an indication of the discontinuous growth. An approximate value for the average cluster radius R can be obtained from the equation[17]

$$\frac{I(\Theta)}{I(0)}=1-n_c\pi R^2\{1+(2/R^2)[\exp(-R/\lambda_e)\times(R\lambda_e+\lambda_e^2)-\lambda_e^2]\} \quad (1)$$

where Θ (Å) is the amount of metal deposited, n_c is the nucleation site density, and $I(0)$ and $I(\Theta)$ are the core-level intensities of the clean substrate and of the substrate with a metal coverage Θ. If we insert in Eq. (1) a typical value of n_c for polycrystalline graphite ($\approx10^{13}\ cm^{-2}$) we obtain $R\approx2\Theta$. The estimate of R is strongly affected by n_c which, in turn, depends on the surface morphology. By transmission electron microscopy, we measured n_c for Pd clusters deposited on an amorphous carbon film supported by a copper mesh and obtained a value of the

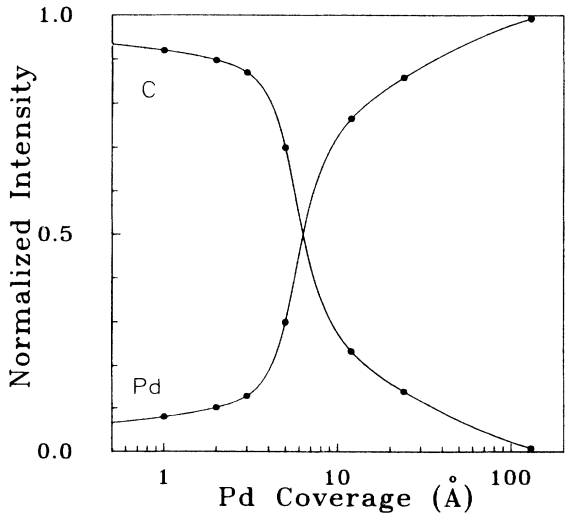

FIG. 1. Percentage ratio of the C $1s$ and Pd $3d$ core-level intensities $[I_{c,Pd}/(I_c+I_{Pd})]$ as a function of the Pd deposition. Core-level intensities are normalized by the XPS sensitivity factors.

same order of magnitude. The above estimates are reliable if interdiffusion effects or compound formation can be excluded. We performed a set of evaporations on the same kind of graphite substrates which were cleaned by Ar-ion bombardment without heating. The behavior of the C and Pd core-level intensities was different from that of Fig. 1. In particular, the presence of large voids in the substrate induced by the ion bombardment, favored a slow progressive interdiffusion of Pd in graphite as a function of time. The most reproducible XPS and AES results are obtained on heated polycrystalline graphite where the roughness of the surface is reduced.

III. THEORETICAL MODEL

We wish to show that the size-dependent spectra which are observed by the various techniques are due to an interplay between one-body effects (due essentially to the mixing of Pd and C orbitals) and many-body complications (due to the partially filled d band). Accordingly, we first review the many-body formalism and demonstrate how the changes in one-electron properties affect the many-body self-energy. Recently, two of us have developed a theory for the photoemission and Auger spectra of partially filled band systems,[18] which generalizes earlier work[19,20] and yields the local density of states (LDOS) with full account for the multiplet structure in the intermediate coupling scheme. The one-electron properties turned out to be much more sensitive to the degree of band filling than the two-hole properties. This prediction is well illustrated here and from a theoretical viewpoint this is perhaps the most interesting point in the present study.

The model Hamiltonian is

$$H=H_0+H_1 \tag{2}$$

where H_0 includes all one-body contributions, including the spin-orbit interaction and

$$H_1=\sum_{JLS} U(LS)|LSJ\rangle\langle LSJ| \tag{3}$$

is the short-ranged part of the Coulomb interaction written in the LSJ picture, where $|LSJ\rangle$ is a two-hole state localized on a site in the lattice. The Coulomb-interaction-matrix elements $U(LS)$ in the Russel-Saunders basis are the energy difference, due to the screened Coulomb interaction, between a two-hole state localized at a given atom and a delocalized two-hole state. The U parameters and the spin-orbit-coupling constant are taken directly from atomic calculations except that the Slater integral F_0 is left as the only adjustable parameter of the theory to allow for the solid-state screening of the interaction. Spin-orbit-projected LDOS computed by self-consistent relativistic (local-density or $X\alpha$) methods may be used to generate the one-body propagators $S(J;\omega)$. There is no double counting of the Coulomb interactions since such methods do not include the diagrams describing the short-range repulsion effects. Hence, one derives the noninteracting two-hole Green's function

$$\phi^0(J_1,J_2;\omega)=\int_{-\infty}^{\infty}\frac{d\omega'}{2\pi}S^0(J_1;\omega')S^0(J_2;\omega-\omega') \ . \tag{4}$$

The self-energy $\Sigma_{\rm LDA}$ is obtained by generalizing Galitzkii's low-density approximation (LDA);[21] however, since Eq. (3) includes the Coulomb interaction at a single site, we must exclude the first-order term, in order to approximately restore the homogeneity of the system. The result reads

$$\begin{aligned}\Sigma_{\rm LDA}(J,\omega)=\tfrac{1}{2}\sum_{J_1J_2J_3}\int_{-\infty}^{\infty}\frac{d\omega'}{2\pi}S^0(J_1;\omega')\\ \times T(J_1JJ_2J_3;\omega+\omega')\\ \times\phi^0(J_2J_3;\omega+\omega')\\ \times W(J_2J_3JJ_1) \ .\end{aligned} \tag{5}$$

Here we have introduced the antisymmetrized Coulomb matrix $W(ijkl)=V(ijkl)-V(ijlk)$, where V is a Coulomb integral, and the $T(\omega)=W[1+(i/2)W\phi(\omega)]^{-1}$ matrix that represents the effective interaction in the partially filled bands. We shall not repeat here the details of the formalism, given elsewhere,[18] and simply note that $\Sigma_{\rm LDA}$ vanishes not only for vanishing W but also for filled bands. In the latter case, all the singularities of the integrand are on the same side of the real axis in the complex plane, and we get the vanishing result by closing the integration contour on the other side.

A. Pd bulk metal

We can apply the above theory to bulk Pd starting from the LDOS calculated by Christensen.[16] Since in palladium the interactions are relatively weak, we assume $T\approx W$ in Eq. (5). Neglecting the energy dependence of the matrix elements, the photoemission bulk Pd spectrum can be approximated to the LDOS which, in turn, is proportional to the real part of the single-particle Green's function $S(J;\omega)$. The result is shown in Fig. 2. The characteristic asymmetry and the main features in the experimental bulk line shape are nicely reproduced. The comparison with the theoretical spectrum obtained with $\Sigma=0$ (dotted line) shows tha correlation effects are essential to understand the *bulk* XPS data.

B. Hole-hole repulsion in supported Pd clusters

Since the dielectric properties depend on particle size[22,23] and particle charging comes into play, the correlation energies U of Eq. (3) in small metal clusters differ from their bulk values. However, no strong variation can be expected here, since the graphite substrate will provide metallic screening and prevent charging. Using a simple approach like a linearized Fermi-Thomas model for a spherical particle[24] one can show that, even for a cluster *in vacuo,* no major change of the W matrix elements should be expected unless the particle size R is so small as to become comparable with the bulk screening length λ.

It is important to realize that the situation is different for free molecules, or *unsupported* clusters which are so

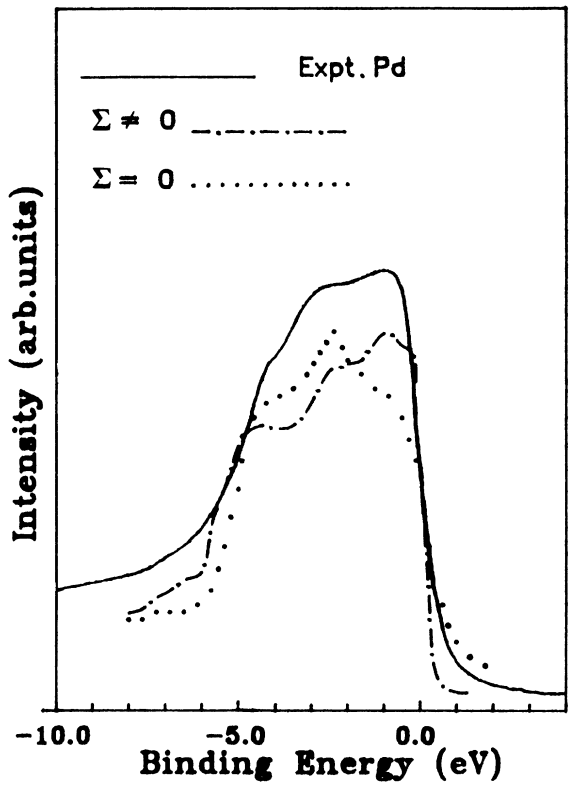

FIG. 2. Bulk Pd XPS spectrum (solid line) and LDOS calculations with self-energy $\Sigma=0$ (dotted line) and $\Sigma\neq 0$ (dashed-dotted line).

small that metallic properties are lost; molecular spectra are properly calculated including a rigid shift by $\langle U\rangle$, and then using[25] $W-\langle U\rangle$ in place of W in the above theory.[26]

For the present supported clusters, however, we shall take the W matrix elements to be size independent.

C. Model LDOS for Pd clusters

Besides the repulsion matrix elements, the uncorrelated one-electron LDOS must be known in order to apply the above theory. Several size-dependent effects must be considered.

An energy shift ΔE_i of the single-particle initial states can be present due to the different electrostatic potential in the bulk and in the cluster.[12,27] Electrostatic effects in the final state can also produce a size-dependent self-energy. Final-states self-energy shifts may be observed with different spectroscopies because of the charge removed or added to the cluster. The substrate is also expected to contribute to the polarization self-energy according to its polarizability. In Sec. IV, however, we shall find empirically that both effects are small and may be neglected in the present case.

Moreover, the LDOS in small clusters can change in a more complicated way because of the large number of surface atoms with lower coordination. In a study of XPS from clusters, Bachelet[11] *et al.* considered the total noninteracting DOS of cubium clusters isolated *in vacuo*. Allowing for surface shifts in the atomic levels they predicted strong deviations from bulk cubium for particles containing $N<10^4$ atoms, which correspond to particle sizes $R<50$ Å. If this effect were important in the present case there would be no simple way to take it into account without a detailed knowledge of particle size and shape distribution and it would require extensive calculations. Fortunately, we shall be able to derive realistic line shapes by ignoring such complications; this indicates that the potential inhomogeneities in our supported particles are effectively screened, and the LDOS at inequivalent Pd sites looks very much the same.

In the following we shall consider the effect of the graphite substrate and evaluate its contribution to the self-energy by a simple phenomenological model. By comparison with the experimental results we will demonstrate that hybridization of the Pd valence d orbitals with the π^* continuum of empty states of graphite is the major effect and it suffices to explain all the trends observed in the experimental data as a function of size and even to give the correct orders of magnitude. All the other effects mentioned above are minor.

The empty states of graphite consist of two main bands π^* and σ^* observed in the BIS spectrum at about 2.5 and 7.5 eV above E_F, respectively. The π^* density of states can be represented with the Gaussian

$$\rho^0(\omega)=\exp[-\Delta(\omega-\omega_0)^2/2] \tag{6}$$

where ω is the energy in eV and $\Delta=0.67$ eV^{-2}. There is then some overlap between ρ^0 and the Pd d band, which implies that the two continua must interact. In the spirit of the Fano-Anderson model, we denote the unperturbed π^* continuum states by the index k and their energy eigenvalues by ε_k. They are connected to the Pd d states by hopping integrals V_{dk}. The local Green's function of Pd d orbitals acquires an extra self-energy

$$\Sigma(\omega)=\Sigma_1(\omega)+i\Sigma_2(\omega)\ , \tag{7}$$

with

$$\Sigma_2(\omega)=\pi\sum_k |V_{kd}|^2\delta(\omega-\varepsilon_k)=\pi\rho^0(\omega)V^2(\omega) \tag{8}$$

and

$$\Sigma_1(\omega)=\int_{-\infty}^{\infty} d\varepsilon\frac{\Sigma_2(\varepsilon)}{\omega-\varepsilon}\ . \tag{9}$$

For the sake of simplicity, we shall consider V^2 as a parameter and neglect its ω dependence. In a microscopic theory, it describes an interaction between the Pd d orbitals and the s-p carbon orbitals. The hybridization is expected to depend on the cluster size; the case $V^2=0$ corresponds to a noninteracting Pd bulk d band and increasing values of V^2 should describe clusters of decreasing size. We can relate the parameter V^2 with the average cluster size R by a simple semiclassical argument. All the electronic levels of the cluster have an energy-dependent finite lifetime $\tau(\omega)$ due to the ability of the electron states to delocalize into the graphite continuum. For an electron at the E_F, $\omega=0$ and we may assume that no effective barrier prevents such a delocalization; therefore

$1/\tau(0) \approx v/R \approx 1/R\sqrt{2W/m}$, where v is the "velocity" and W is the band width ($W \approx 6$ eV ≈ 0.22 a.u.). The lifetime broadening at the Fermi level is $\approx \Sigma_2(\omega=0) \approx 0.122\pi V^2$. Equating this to $v/R \approx 9/R(\text{Å})$ eV, we obtain

$$V^2 \approx \frac{23}{R(\text{Å})}\ \text{eV}^2 . \tag{10}$$

In order to show the qualitative effect of the interaction between the continua, we first use a simplified model for the Pd d band given by a triangular DOS. The local single-particle Green's function is written as

$$G^0(\omega) = G_1^0 + iG_2^0 , \tag{11}$$

$$G_1^0 = \frac{2}{T-B}\left[\frac{\omega-B}{C-B}\ln\left|\frac{|B-\omega|}{|C-\omega|}\right| + \frac{T-\omega}{T-C}\ln\left|\frac{|C-\omega|}{|T-\omega|}\right|\right] , \tag{12}$$

$$G_2^0 = \frac{2\pi}{T-B}\left[\frac{\omega-B}{C-B}\Theta(\omega-B)\Theta(C-\omega) + \frac{T-\omega}{T-C}\Theta(\omega-C)\Theta(T-\omega)\right] \tag{13}$$

with the band bottom $B=-5.6$ eV, the band top $T=0.56$ eV, and the maximum $C=(T+B)/2$. The interaction with graphite is then included via Dyson's equation

$$G = \frac{G^0}{1-G^0\Sigma} . \tag{14}$$

The effects of Σ on the Pd LDOS ρ^0 in the absence of correlation effects are shown in Fig. 3 for several values of V^2. The case $V^2=0$ represents our simplified version of LDOS for bulk Pd, with the Fermi level at $\omega=0$. If the G propagator were inserted into the theory described for Pd bulk bands, the Σ_{LDA} correlation would induce a shift of the maximum of the occupied DOS towards the Fermi level, while the unoccupied states would undergo minor modifications. For $V^2=0.5$, we observe a resonance centered at about 2.3 eV above the Fermi level. It corresponds to hybrid empty states having d character inside the cluster and π^* character on the substrate. The main line shape of the occupied DOS is not qualitatively modified, but the DOS near the Fermi level is reduced. With increasing V^2, a gap develops between the resonant hybrid state and the occupied states, and the occupied band becomes completely filled. In this way, Σ_{LDA} is drastically reduced, the correlation-induced features vanish, and the line shape becomes symmetric as for the bulk Pd spectrum of Fig. 2 calculated for $\Sigma_{\text{LDA}}=0$. For $V^2=3$, which corresponds to very small clusters, even the main line shape is appreciably distorted, with the maximum shifting at higher binding energies. We remark that the reduction of Σ_{LDA} with reducing R cannot be justified by a reduction of the U parameters, for the reasons mentioned above, but has to be assigned to the Pd d states hybridizing with the graphite states and becoming bonding. Concomitantly, the antibonding hybrid resonance becomes sharper and shifts higher in energy. Hence we conclude that we may expect to see a suppression of Σ in the small particles; however, this is *not due to a vanishing hole-hole interaction, but to the relaxation being inhibited because of the filling of the valence band.* Qualitatively, this is consistent with the notion that the $4d^{9.6}$ configuration of Pd metal should tend to the $4d^{10}$ free-atom configuration.

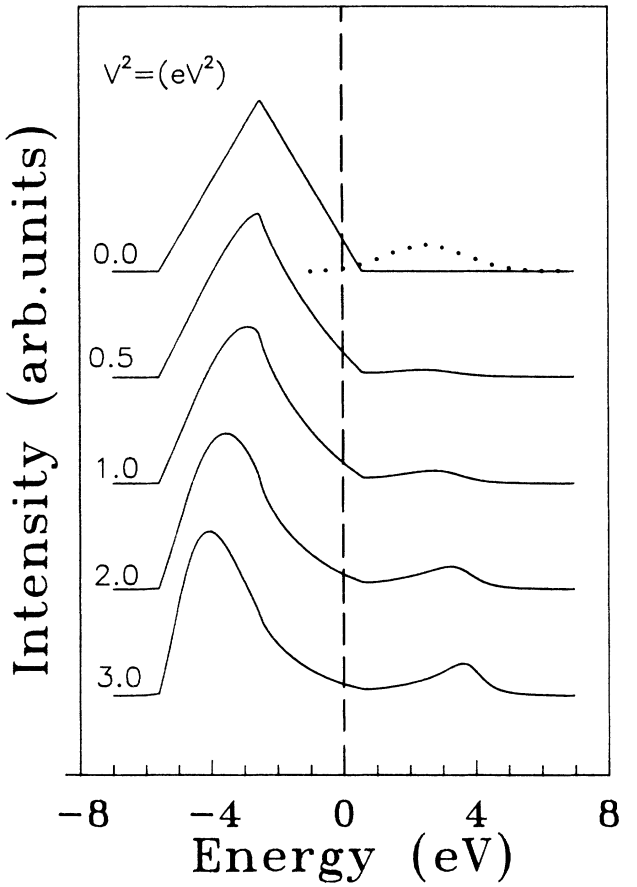

FIG. 3. Cluster model applied to a simplified version of the uncorrelated PD LDOS to show the effect of the hybridization with the graphite empty π^* band (dotted curve) described by the parameter V^2 (see sec. III C for details).

Now we wish to show how the above model explains not only the photoemission line shapes, but all the other spectra as well.

IV. RESULTS AND DISCUSSION

For a closer comparison with the experimental data we apply the above formulation to a realistic description of the $4d$ bands of Pd by using Christensen's J-resolved theoretical LDOS's (Ref. 16) $N_j(\omega)$. This is normalized by

$$\int d\omega\, N_j(\omega) = 1 \quad \text{for } j = \tfrac{3}{2}, \tfrac{5}{2}$$

and is related to the one-body noninteracting propagator by

$$G_j(\omega)=\int d\omega' N_j(\omega')[\omega-\omega'+i\delta\,\mathrm{sign}(\omega')]^{-1} \quad (15)$$

with $\delta\to 0$. These are then used in the full intermediate-coupling theory. All the values of the parameters, like Slater's integrals, multiplet splittings, lifetime broadening, etc., are *bulk* values.

A. XPS spectra

Figure 4 shows a comparison between valence band photoemission spectra for increasing (nominal) thicknesses of Pd deposited on graphite and calculated XPS curves for different V^2 values. It may be noticed that the line shapes depend remarkably on particle size, and while the biggest particles show the characteristic bulklike profile, the smaller ones show a reduction in the density of states at E_F and have a much more symmetrical d band. With decreasing cluster size the valence band centroid shifts to higher binding energy by about 0.6 eV accompanied by a parallel displacement of the Pd $3d$ core levels. Notice the striking similarity between the spectra labeled 14 and 7 Å in Fig. 4 and the one computed for $\Sigma=0$ in Fig. 1. This is an indication that, with reducing particle size, the spectra simply evolve as if Σ were reduced. There is a remarkably good agreement between the experimental data taken as a function of size and the predictions of the model as function of the parameter V^2, considering that our phenomenological model describes with a single parameter an inhomogeneous situation due to a distribution of particle sizes.

Despite the experimental uncertainties, it can be seen in Fig. 4 that the R^{-1} dependence of V^2 is a reasonable approximation and leads to R values proportional to the nominal film thicknesses.

B. AES spectra

Further support for the conclusion that a size effect on Σ_{LDA}, rather than the W matrix of Eq. (5), plays the dominant role, comes from the analysis of the $M_{4,5}NN$ Auger

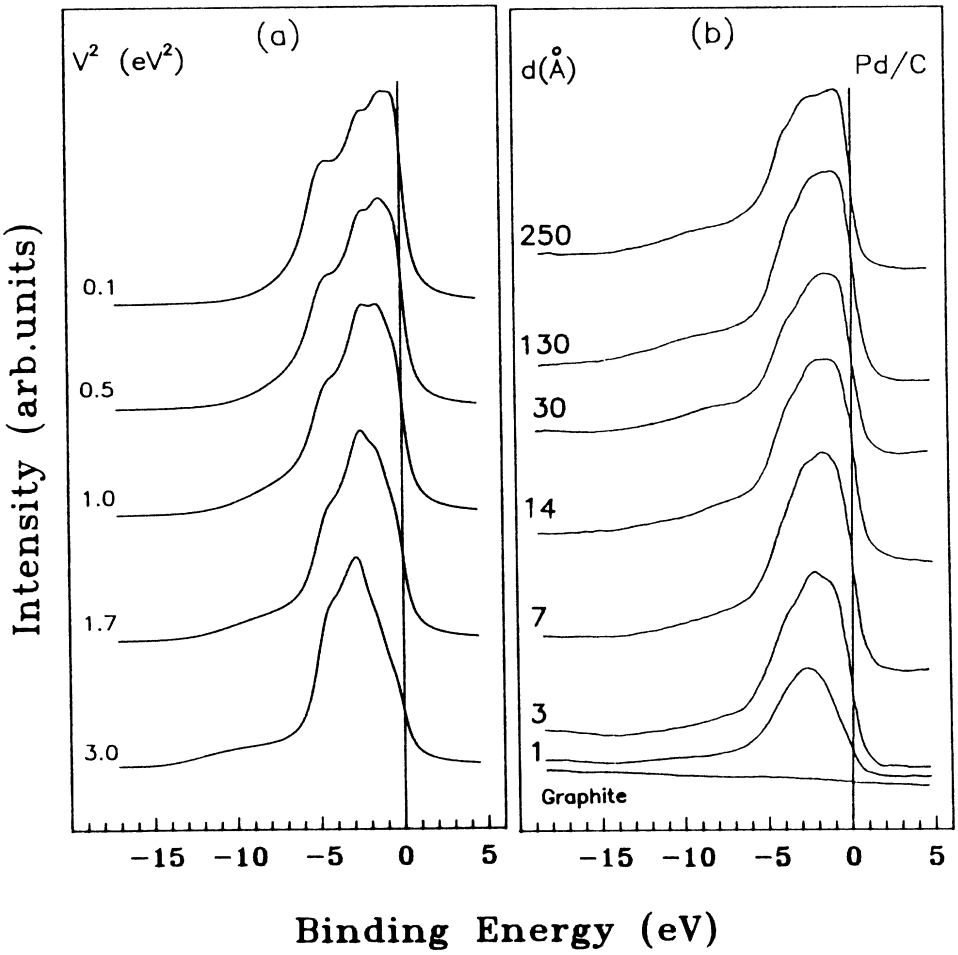

FIG. 4. XPS valence band spectra of Pd clusters on polycrystalline graphite for different nominal Pd thicknesses (b) and theoretical curves (a) calculated using the cluster model, presented in Sec. III C, applied to Christensen's Pd LDOS of Ref. 16.

spectra of Fig. 5(b). The two main structures are the contributions of the $3d_{3/2}$ and $3d_{5/2}$ primary holes split by 5.3 eV. The observation that the line shape is not appreciably modified in clusters is an indication that W does not undergo sizable changes. An almost rigid shift by about 1 eV to lower kinetic energy is measured for the smallest particles. The initial core hole of the Auger process can be affected, with decreasing cluster size, by an initial-state shift ΔE_i due to differences in the potential and by a shift C due to the change in Coulomb and polarization energy which includes the contribution of the substrate.[28] The two-hole final state is expected to shift by $4C$, therefore the shift of the Auger spectrum should be $3C$. Taking into account the ≈ 0.5-eV energy difference measured for the Pd $3d$ binding energy, we can conclude that both ΔE_i and C are quite small (≈ 0.25 eV).

On the other hand the vanishing of Σ_{LDA} will not greatly affect the spectra since the two localized final holes are essentially bare holes, and in fact Auger line shapes are computed in the "bare-ladder approximation" suitable for almost-filled bands.[29] The Auger yield is given by

$$A(\omega)=\pi^{-1}\sum_j\sum_\lambda I(\lambda_j)\mathrm{Re}\phi^j_{\lambda\lambda}(\omega) \tag{16}$$

where $I(\lambda_j)$ and λ_j are, respectively, atomic intensities and eigenvectors calculated in the intermediate-coupling scheme for the d^8 configuration and the Green's-function matrix $\phi^j_{\lambda\lambda}(\omega)$ is written in terms of the uncorrelated two-particle Green's function ϕ^j_0 which is related to the $G^0_{3/2}$ and $G^0_{5/2}$ spin-orbit-projected single-particle propagators of Eq. (15). The dependence of G_j on V^2 is introduced through the self-energy Σ in Eq. (14). To account for lifetime effects and experimental resolution a Lorentzian broadening (full width at half maximum of 0.9 eV) has been added. Figure 5(a) shows the calculated Auger spectra and their dependence on V^2 parameters. We observe that the model is capable of reproducing the experimental trends in great detail, including the progressive disappearance in small clusters of the shoulder on the low kinetic energy side of the main peak and the increase in intensity of the main peak with respect to the shoulder on its high kinetic energy side.

The sharpening of the structures on going to higher V^2 values reflects a less bandlike behavior of the line shape because the occupied part of the $4d$ LDOS is reduced by hybridization with the π^* orbitals. A slightly larger energy shift is predicted by the theory for small clusters. The discrepancy can be related to the inhomogeneities in the size distribution whose effect is more evident at very low Pd depositions.

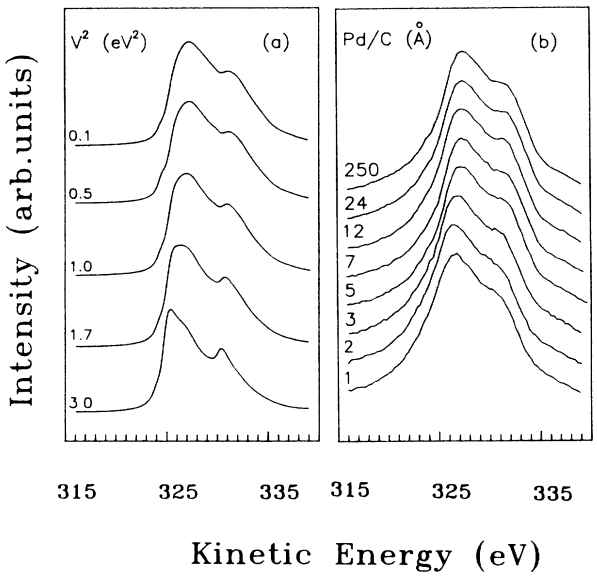

FIG. 5. $M_{4,5}NN$ Auger spectra of Pd clusters on polycrystalline graphite for different nominal Pd thicknesses (b) and calculated line shapes (a) in the "bare-ladder approximation" (see Sec. IV. B using the cluster model presented in Sec. III C.

C. BIS spectra

In Fig. 6 is shown a set of BIS spectra taken at different Pd thicknesses. The spectrum labeled 250 Å can be assumed to be representative of bulk Pd and reflects the d projection of the empty DOS in agreement with the L_2

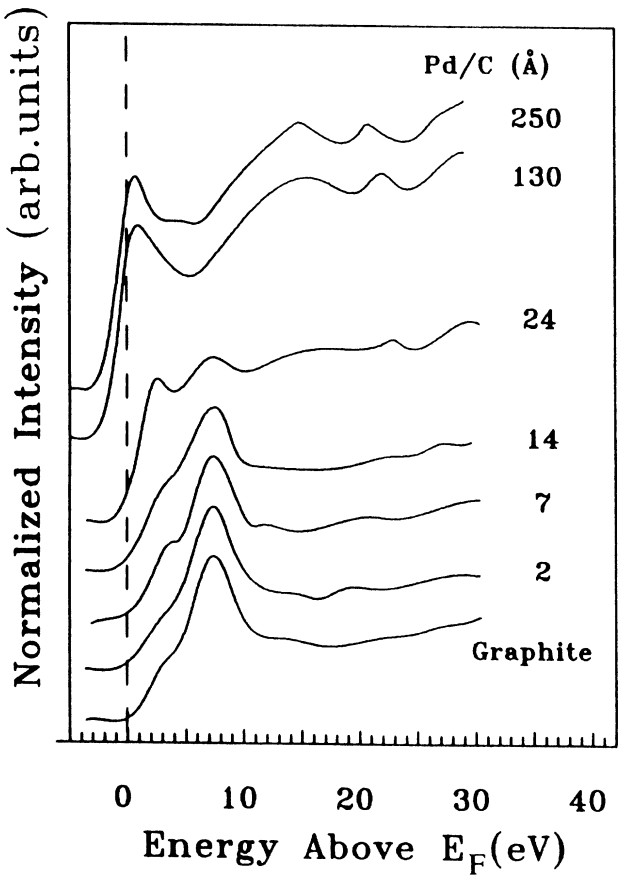

FIG. 6. BIS spectra of Pd clusters on polycrystalline graphite for different nominal thicknesses.

absorption edge of bulk Pd (Ref. 5) shown in Fig. 8(b). At the bottom of Fig. 6 we report the spectrum of clean graphite which consists of two structures at +2.5 and +7.5 eV assigned, respectively, to transitions to the π^* and σ^* empty bands.[30] With increasing cluster size, the spectrum gradually modifies until the bulk Pd line shape is reached. The evolution of the spectra is better evidenced in Fig. 7(b) where the contribution of the clean graphite spectrum was subtracted. This procedure which implies a careful alignment of the Fermi energies has been described in detail elsewhere.[31] The two top curves of Fig. 7(b) are the same as in Fig. 6 while the three bottom ones are difference curves (dashed lines). A band of hybrid states initially located at ≈ 3.2 eV moves toward E_F by 3.5 eV, with increasing cluster size, to match the position of the main d band of bulk Pd at ≈ 0.7 eV above E_F.

To derive an approximate expression for the BIS amplitude suitable for a complicated inhomogeneous system we proceed as follows. The BIS transition is determined by the matrix elements of the $\mathbf{A}\cdot\mathbf{p}$ interaction between the initial electron state $\mathbf{p}_0$ and the final state ν in the solid. When ν is analyzed in terms of atomic empty orbitals in a tight-binding picture and the transition probability is written down according to the Fermi golden rule, interference terms arise between different sites. However, in the present experiments 1500-eV electrons were used, and $\mathbf{p}_0$ may be taken to be a plane-wave state of such a short wavelength that interference terms are effectively suppressed. Then, the BIS cross section becomes

$$\sigma(E)\approx \sum_i I_i \sigma_i^{\mathrm{at}}(E) , \tag{17}$$

that is, a sum of independent contributions from all sites in the system, weighted by their atomic transition probability and by the intensity I of the electron beam at each site. Since $\sigma_i^{\mathrm{at}}(E)$ is proportional to the LDOS at site i, the BIS signal can be regarded as a weighted average of the LDOS at the sites which are seen by the beam. Therefore, in order to simulate the difference spectra of Fig. 7(b), we start with the Pd LDOS

$$\rho(\omega)=-\left[\frac{1}{\pi}\mathrm{Im}G\right] , \tag{18}$$

and cut out the occupied portion of the LDOS. The resulting line shape is broadened to account for the 1.1-eV experimental resolution.

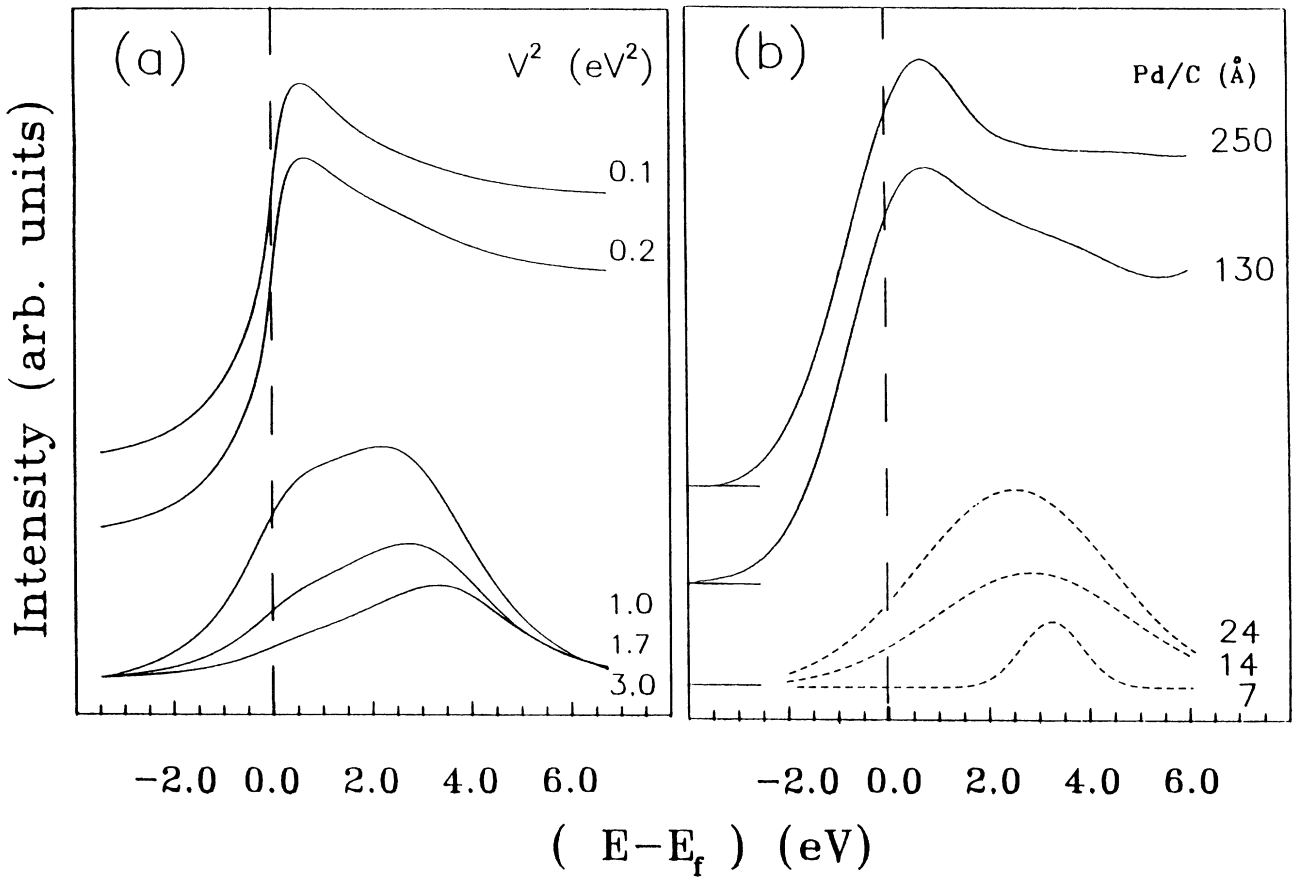

FIG. 7. Calculated BIS spectra for Pd clusters on graphite (a) and comparison with the experiment (b). The $V^2=0.1$ and $V^2=0.2$ theoretical curves are weighted by the Pd BIS matrix elements. The spectra labeled 7, 14, and 24 Å [dashed lines (b)] are difference curves obtained by subtracting the BIS spectrum of clean graphite.

The results for various V^2 values are displayed in Fig. 7(a). The $V^2=0.1$ and $V^2=0.2$ curves, that according to Eq. (10), should roughly correspond to the 250- and 130-Å spectra, respectively, have been weighted with the calculated BIS matrix elements.[32] In the $V^2=0.2$ curve, an incipient high-energy shoulder corresponding to the hybrid resonant states is predicted and this structure is indeed born out by the experimental data. With increasing V^2, the hybrid resonance increases and becomes dominant, while the maximum shifts to higher energies. In fact, the BIS difference data labeled 24 Å do not show any sign of a two-peak structure and reach a maximum at 2.5 eV. We expect them to correspond to $V^2\approx 1$, and, in fact, the line-shape simulation is quite good, and the maximum occurs at the correct position. The calculated width at half maximum (4.5 eV) agrees with the measured one (4.45 eV). For the 14-Å particles the measured width is the same and the maximum is at 2.85 eV; choosing $V^2=1.7$ we obtain the same width and the maximum at 2.76 eV. Finally, for the 7-Å particles the experimental maximum is at 3.2 eV. This agrees well with the calculations for $V^2=3$, which is still remarkably close to the value predicted by Eq. (10). The experimental data suggest a narrowing of the peak, and the hybrid resonance also becomes narrower. We conclude, therefore, that our model is in semiquantitative agreement also with the BIS data.

D. XANES spectra

X-ray absorption, contrary to the spectroscopies discussed above, leaves the total number of electrons unchanged in the cluster. Charging effects are, then, expected to be absent. Figure 8(b) shows the measured L_2 absorption threshold for bulk Pd and for a cluster of approximately 14 Å supported on graphite.[33] Note the shift of the main peak which is of the same order of magnitude ($\sim$2eV) and in the same direction as that measured by BIS, a further confirmation that strong final-state effects must be ruled out.

To interpret the XANES data we look for a first approximation to the golden-rule expression for the cross section

$$\sigma(\omega)=K\sum_{\nu}|\langle c|\,\mathbf{A}\cdot\mathbf{p}|\nu\rangle|^2\delta(\omega-\varepsilon_\nu) \tag{19}$$

where K is a constant, c denotes the core-hole state, and ν denotes the final-state electronic states in the presence of the core hole. Taking the selection rules into account, and neglecting the contribution of s states, we may write, in a tight-binding model,

$$\langle c|\,\mathbf{A}\cdot\mathbf{p}|\nu\rangle=\sum_{n>3}\langle c|\,\mathbf{A}\cdot\mathbf{p}|nd\rangle\langle nd|\nu\rangle \tag{20}$$

where nd denote the Pd d orbitals with $n\geq 4$. As far as the different d bands do not overlap in energy, we get

$$\sigma=K\sum_{n}|M_{nd}|^2\rho_{nd}(\omega)\ , \tag{21}$$

where M are atomic matrix elements and ρ is a LDOS computed in the presence of the core hole. In practice, when we describe the first few eV above threshold, we forget about the d bands with $n>4$. For computing ρ, we can use the equivalent core approximation. Since the

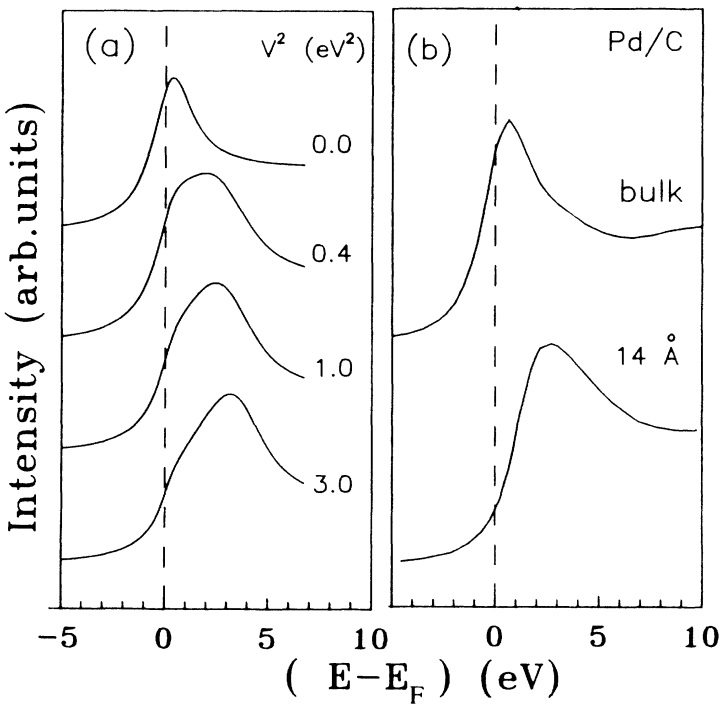

FIG. 8. Comparison between the theoretical XANES spectra for Pd clusters of increasing size deposited on graphite (a) and the XANES data of De Crescenzi *et al.* (Ref. 5).

d states in the Ag atom are more strongly bound than in Pd by $\Delta\varepsilon = 1.66$ eV, we use this $\Delta\varepsilon$ to modify the local Pd Green's function according to the Wolff-Clogston prescription[34]

$$G \rightarrow \frac{G}{1-\Delta\varepsilon G} \ . \tag{22}$$

In this way, the hybrid resonance is affected by the core-hole potential and the admixture of d and π^* components is different than in the BIS experiment, leading to a different line shape. The evolution of the XANES simulation with increasing V^2 is illustrated in Fig. 8(a). To improve the comparison with the experiments, a background was added to the calculated curves, proportional to $\arctan[2(h\omega - E_F)/\Gamma]$ where Γ is the core-hole linewidth. It may be noted that the model predicts different line shapes for BIS and XANES at small V^2, that is for larger clusters, while for V^2 of order 1 or more the shapes are rather similar, and the maxima occur at slightly lower energy in XANES. The near coincidence of the maxima, which we mentioned above to rule out a major effect of screened Coulomb self-energy, is indeed accounted for by the present model. Moreover, the 4.5-eV linewidth is well reproduced by the model. The only data available refer to clusters of average size $R = 14$ Å; since, however, the cluster sizes were determined by a different method in this experiment,[33] we cannot be sure of the absolute position of these clusters in the size scale of the others. However, if we assume that they were about the same as the 7-Å clusters of the BIS experiment, which were well described by $V^2 = 3$ eV^2, we predict a maximum at about 3 eV above the Fermi level, while the experimental maximum is at 2.2 eV. Thus, while we understand the shift from the bulk white line qualitatively, we cannot reach the same quantitative accuracy as in the BIS case. A possible explanation is that larger particles in the size distribution would shift the maximum to lower energy and their weight in the XANES spectrum should be greatly enhanced due to the increase in the x-ray-absorption cross section with increasing particle size. The latter point is, at present, not understood. Our model predicts that with reducing R the hybridization should be enhanced, leaving more d states available to the XANES transition and enhancing the intensity. We believe that there is a good deal of evidence in favor of the present model, and in order to understand absolute intensities we would need a far more refined treatment of the XANES cross section, allowing for several bands. Such developments are outside the scope of the present paper.

V. CONCLUSIONS

In summary, we find that in clusters of partially filled band metals such as Pd deposited on graphite, the changes observed in the electronic structure, as a function of the particle average size, can be fully understood in terms of the interaction with the substrate. Initial-state energy shifts and cluster charging are estimated to be not larger than 0.25 eV, for the present system.

A simple phenomenological model is introduced in which Pd $4d$ filled bands and π^* empty graphite states strongly hybridize in the Fermi energy region. The bulk Pd density of states is modified by the extra contribution to the self-energy introduced by the graphite. The interaction between Pd d orbitals and carbon s-p orbitals is described by the parameter $V^2 \propto R^{-1}$. As a consequence a band of hybrid states arises above E_F. With decreasing cluster size, a 2-eV energy shift of the hybrid states and the opening of a gap occur, as observed both in BIS and XANES spectra. The Pd valence d band fills up and correlation-induced features disappear from XPS spectra.

The model is able to closely follow, as a function of the cluster average size, line-shape changes and energy shifts in XPS, AES, and BIS; a fairly good description is obtained also for XANES spectra. A coherent and unified picture of occupied and empty-state spectroscopies emerges. We expect a similar description to be relevant and other d-band metals on substrates having high densities of states a few eV above the Fermi level.

ACKNOWLEDGMENTS

We thank G. Mattogno, C. Battistoni, and P. Fiordiponti of the Area di Ricerca di Roma–Montelibretti of the Consiglio Nazionale delle Ricerche for the supply of the monochromator for BIS measurements. This research has been partially supported by the Italian CISM-GNSM. M.S. would like to thank the International Centre for Theoretical Physics for partial financial support.

*Permanent address: GPS-ENS, Université Paris VII, 75251 Paris, France.

[1]H. Poppa, Vacuum **34**, 3786 (1986).
[2]M. G. Mason, Phys. Rev. B **27**, 748 (1983).
[3]G. K. Wertheim, S. B. Di Cenzo, and D. N. E. Buchanan, Phys. Rev. B **33**, 5384 (1986).
[4]S. Kohiki and S. Ikeda, Phys. Rev. B **34**, 3786 (1986).
[5]M. De Crescenzi, M. Diociaiuti, P. Picozzi, and S. Santucci, Phys. Rev. B **34**, 4334 (1986).
[6]E. F. Egelhoff, Jr. and G. G. Tibbetts, Solid State Commun. **29**, 53 (1979).
[7]S. Ichikawa, H. Poppa, and M. Boudart, J. Catal. **91**, 1 (1985).
[8]M. G. Mason, L. J. Gerenser, and S. T. Lee, Phys. Rev. Lett. **39**, 288 (1977).
[9]G. K. Wertheim, S. B. Di Cenzo, D. N. E. Buchanan, and P. A. Bennett, Solid State Commun. **53**, 377 (1985).
[10]F. Parmigiani, E. Kay, P. S. Bagus, and C. J. Nelin, J. Electron Spectrosc. Relat. Phenom. **36**, 257 (1985).
[11]G. B. Bachelet, F. Bassani, M. Bourg, and A. Julg, J. Phys. C **16**, 4305 (1983).
[12]E. F. Egelhoff, J. Vac. Sci. Technol. **20**, 668 (1982).
[13]B. Frick and K. Jacobi, Surf. Sci. **178**, 907 (1986).
[14]I. Abbati, L. Braicovich, C. M. Bertoni, C. Calandra, and F. Manghi, Phys. Rev. Lett. **40**, 469 (1978).

[15]F. Houzay, G. M. Guichar, A. Cros, F. Salvan, R. Pinchaux, and J. Derrien, J. Phys. C **15**, 7065 (1982).
[16]N. E. Christensen, J. Phys. F **8**, L51 (1978).
[17]Y. Hu, T. J. Wagner, W. Gao, H. M. Meyer III, and J. H. Weaver, Phys. Rev. B **38**, 3037 (1988).
[18]M. Cini and C. Verdozzi, in *Auger Spectroscopy and Electronic Structure,* Vol. 18 of *Springer Series in Surface Science,* edited by G. Cubiotti, G. Mondio, and K. Wandelt (Springer-Verlag, Berlin, 1989), p. 122.
[19]M. Cini, Solid State Commun. **20**, 605 (1976); **24**, 681 (1977); G. A. Sawatzky, Phys. Rev. Lett. **39**, 504 (1977); G. A. Sawatzky and A. Lenselink, Phys. Rev. B **21**, 1790 (1980).
[20]M. Cini, Surf. Sci. **87**, 483 (1979); D. R. Penn, Phys. Rev. Lett. **42**, 921 (1979); A. Liebsch, *ibid.* **43**, 1431 (1979); Phys. Rev. B **23**, 5203 (1981); V. Drchal and J. Kudrnowsky, J. Phys. F **14**, 2443 (1984).
[21]V. Galitzkii, Zh. Eksp. Teor. Fiz. **34**, 151 (1958) [Sov. Phys.—JETP **7**, 104 (1958)].
[22]M. Cini and P. Ascarelli, J. Phys. F **4**, 1998 (1974).
[23]M. Cini, Surf. Sci. **62**, 148 (1977).
[24]P. Ascarelli and M. Cini, in *Emission and Scattering Techniques in the Study of Inorganic Molecules, Solids and Surfaces, NATO Advanced Study Institute,* edited by P. Day (Reidel, Dordrecht, Holland, 1981).
[25]T. D. Thomas and P. Weightman, Chem. Phys. Lett. **81**, 325 (1981).
[26]M. Cini, F. Maracci, and R. Platania, J. Phys. (Paris) Colloq. Suppl. **12**, 48, C9-781 (1987).
[27]E. F. Egelhoff, Surf. Sci. Rep. **6**, 253 (1986), and references therein.
[28]Despite the conducting nature of the substrate, a shift C should affect the valence states as well, because the Auger spectrum reflects a local DOS.
[29]C. Verdozzi, thesis, Università di Roma "La Sapienza," 1985 (unpublished); M. Cini and C. Verdozzi, Solid State Commun. **57**, 657 (1986); Nuovo Cimento **9D**, 1 (1987); J. Phys. Condensed Matter, **40**, 7457 (1989).
[30]V. Dose, G. Reusing, and H. Scheidt; Phys. Rev. B **26**, 984 (1982).
[31]M. De Crescenzi, F. Patella, N. Motta, M. Sastry, F. Rochet, R. Pasquali, and A. Balzarotti, Solid State Commun. **73**, 251 (1990).
[32]W. Speier, J. C. Fuggle, P. Durham, R. Zeller, R. J. Blakes, and P. Sterne, J. Phys. C **21**, 2621 (1988).
[33]The experimental data are taken from Ref. 5.
[34]P. A. Wolff, Phys. Rev. **124**, 1030 (1961); A. M. Clogston and P. W. Anderson, Bull. Am. Phys. Soc. **6**, 124 (1961).